



## SYMPOSIUM

# Size-Dependent Scaling of Stingless Bee Flight Metabolism Reveals an Energetic Benefit to Small Body Size

Meghan E. Duell \*<sup>1</sup>, C. Jaco Klok †, David W. Roubik ‡ and Jon F. Harrison †<sup>1</sup>

\*Department of Biology, Western University, 1151 Richmond Street, London, ON N6A 5B7, Canada; <sup>†</sup>School of Life Sciences, Arizona State University, Tempe, AZ 85287-4501, USA; <sup>‡</sup>Smithsonian Tropical Research Institute, Luis Clement Avenue, Bldg. 401 Tupper, Balboa Ancon, Panama City, Republic of Panama

From the symposium “Causal mechanisms of interspecific metabolic scaling patterns” presented at the annual meeting of the Society for Integrative and Comparative Biology virtual annual meeting, January 3–February 28, 2022.

<sup>1</sup>E-mail: [mduell@uwo.ca](mailto:mduell@uwo.ca) (MED); [j.harrison@asu.edu](mailto:j.harrison@asu.edu) (JFH)

**Synopsis** Understanding the effect of body size on flight costs is critical for the development of models of aerodynamics and animal energetics. Prior scaling studies that have shown that flight costs scale hypometrically have focused primarily on larger (>100 mg) insects and birds, but most flying species are smaller. We studied the flight physiology of 13 stingless bee species over a large range of body sizes (1–115 mg). Metabolic rate during hovering scaled hypermetrically (scaling slope = 2.11). Larger bees had warm thoraxes, while small bees were nearly ectothermic; however, even controlling for body temperature variation, flight metabolic rate scaled hypermetrically across this clade. Despite having a lower mass-specific metabolic rate during flight, smaller bees could carry the same proportional load. Wingbeat frequency did not vary with body size, in contrast to most studies that find wingbeat frequency increases as body size decreases. Smaller stingless bees have a greater relative forewing surface area, which may help them reduce the energy requirements needed to fly. Further, we hypothesize that the relatively larger heads of smaller species may change their body pitch in flight. Synthesizing across all flying insects, we demonstrate that the scaling of flight metabolic rate changes from hypermetric to hypometric at ~58 mg body mass with hypermetric scaling below (slope = 1.2) and hypometric scaling (slope = 0.67) >58 mg in body mass. The reduced cost of flight likely provides selective advantages for the evolution of small body size in insects. The biphasic scaling of flight metabolic rates and wingbeat frequencies in insects supports the hypothesis that the scaling of metabolic rate is closely related to the power requirements of locomotion and cycle frequencies.

## Introduction

Understanding how body size affects animal function is one of the central themes of biology; such scaling studies have provided key syntheses of organismal function and macroecology (Sibley *et al.* 2012). Flight is a key trait for the evolutionary success of insects, birds, and bats, being integral to resource collection (pollination), migration, and defense. The scaling of flight metabolic rate with mass in insects remains a controversial issue. Studies of hovering moths and bees ranging in mass from 100 to 1100 mg have shown that flight metabolic rates scale hypometrically (slope < 1, indicating lower energy use per gram body

mass in larger animals compared with smaller animals) with slopes of log metabolic rate on log mass of 0.63–0.77, with wing beat frequencies consistently shown to decline in larger insects (Bartholomew and Casey 1978; Suarez 2000; Darveau *et al.* 2005). In contrast, a meta-analysis by Niven and Scharlemann (2005) suggested that across all insects, flight metabolic rate scales hypermetrically (slope > 1, indicating greater energy use per gram body mass in larger animals compared with smaller animals) with mass<sup>1.1</sup>, and that this was due to insects <10 mg in mass having distinctly lower flight metabolic rates than insects above this size (Casey *et al.* 1985). However, these authors

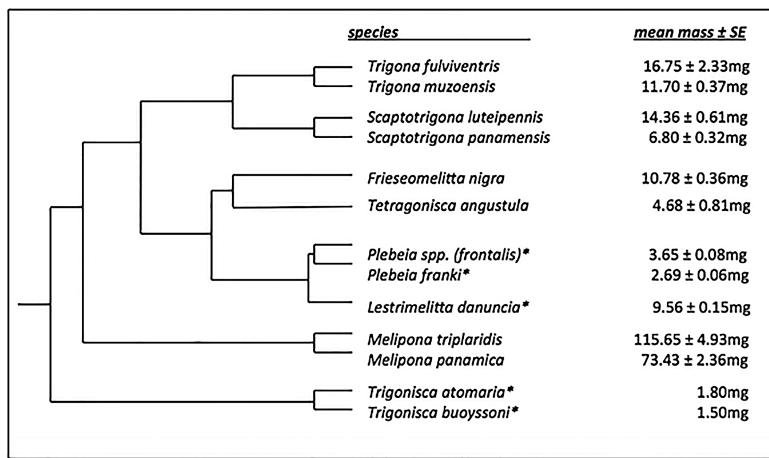


**Fig. 1** Phylogenetic tree of stingless bee species included in this study based on relationships found in Rasmussen and Cameron 2007, 2010. All branch lengths are set equal to 1 because of the absence of some species from available molecular phylogenies of Meliponines. Phylogenetic independent contrasts demonstrate that phylogeny is not a significant factor in our analysis (Table 1). *Plebeia* spp. (*frontalis*) is undescribed. PGLS analysis was done with and without this species included and did not yield different results. Average body mass ± SE are indicated next to species names and miniaturized lineages are specified with an asterisk according to Michener (2001) and de Camargo (2013).

noted that their conclusions were hampered by a dearth of studies of insect flight in the size classes across which flight costs seem to change dramatically (10–100 mg).

We aimed to determine how and why the scaling of flight metabolic rate changes with body mass among insects using stingless bees as a subset of small flying insects. The mechanisms causing hypometric scaling of metabolic rate are controversial. Supply constraint hypotheses, such as the idea that limitations on gas or nutrient transport occur due to decreasing surface-to-volume ratios or the fractal nature of delivery systems, imply that consistent hypometric scaling should be observed (Nisbet et al. 2000; West et al. 2000; Cardoso et al. 2006). Conversely, the idea that the energetic costs of locomotion drive metabolic scaling suggest that a primary driver of hypometric scaling of metabolic rate in animals is the decline in cycle frequency observed in larger runners, swimmers, and fliers (Biewener and Patek 2018). Declining cycle frequency lowers cost because the rate of myosin ATPase activity increases with muscle contractile speed and contractile frequency, and likely elastic energy storage also decreases (Biewener and Patek 2018). In most flying insects that have been examined, wing-beat frequency declines in larger species, as found in birds and bats (Casey 1989; Harrison and Roberts 1998; Darveau et al. 2005). Whether these trends in wingbeat frequency occur across smaller insect fliers is unknown.

We measured flight metabolic rates, wingbeat frequency, voluntary load carriage, and wing and body segment sizes in 13 species of stingless bees between 1.5 and 115 mg. We used stingless bees (Meliponini)

for these measurements because they have a large range of body size among species, ~1–150 mg (Figs. 1 and 2A) with a well-defined molecular phylogeny (Felsenstein 1985; Harvey and Pagel 1991; Ramírez et al. 2010; Rasmussen and Cameron 2010). Some lineages, especially the genus *Melipona*, have large species ranging in body mass up to 150 mg (de Camargo 2013). Miniaturization has evolved multiple times among 33 genera (Michener 2001; de Camargo 2013) and it is thought that ancestral Meliponines were moderately sized, perhaps 50 mg (Ramírez et al. 2010; Rasmussen and Cameron 2010; de Camargo 2013; de Camargo and Pedro 2013). The smallest species we used, *Trigonisca buoysonni*, was 1.5 mg in size, while the largest, *Melipona triplaridis*, was 115 mg ± 5 mg. Additionally, most stingless bees fill a similar ecological niche regardless of body size; all are social, living in colonies with task differentiation, and most forage on flowers resulting in a pollen and nectar diet. This diversity in the evolution of body size across the phylogeny of stingless bees and similar ecologies makes them ideal for comparative work.

## Materials and methods

**Study sites and stingless bee collection:** Stingless bee foragers from 11 species (*M. triplaridis*, *M. panamica*, *Scaptotrigona panamensis*, *S. luteipennis*, *Trigona fulviventris*, *T. muzoensis*, *Tetragonisca angustula*, *Friesomelitta nigra*, *Lestrimelitta danuncia*, *Plebeia franki*, *P. frontalis*) were captured returning to nests at several locations in the Republic of Panamá. *Scaptotrigona lutipennis*, *T. angustula*, *F. nigra*, and *T. fulviventris*

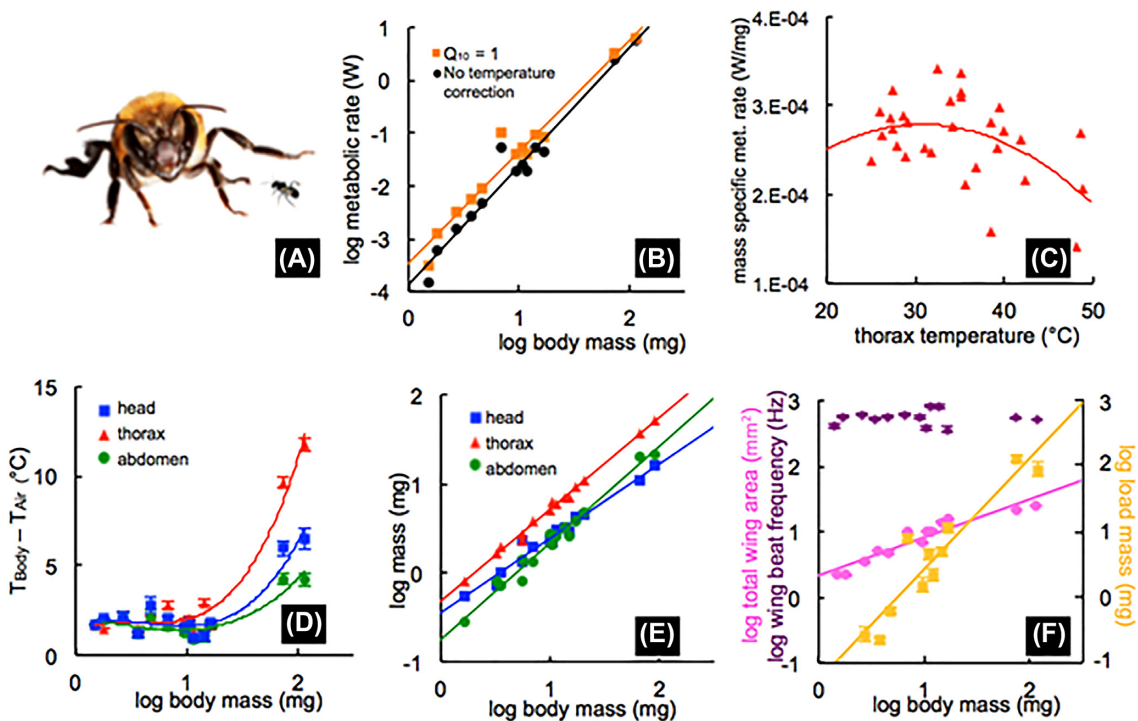


**Fig. 2** (A) Size comparison of biggest and smallest stingless bees included. (B) Metabolic rates of stingless bees with and without  $Q_{10}$  correction of 2. Line shows a second-order polynomial fit. (C) The thermal flight performance curve of *S. luteipennis* ( $n = 30$ ) indicates that  $Q_{10}$  for this stingless bee is  $\approx 1$ . (D) Body segment temperature elevation above air temperature (23.5–25.5°C). Small bees ( $< 20$  mg) had body temperatures 0.7–3°C above air temperatures, while large species ( $> 70$  mg) had substantially elevated body segment temperatures. Lines show third-order polynomial fits. (E) Thorax mass scaled isometrically, head mass scaled hypometrically, and abdomen mass scaled hypermetically (slope = 1.05 for thorax, 0.86 for head, and 1.11 for abdomen) across stingless bees. (F) Wingbeat frequency was constant across body size, while load carriage abilities scaled isometrically (slope = 1.05). Total wing area scaled hypometrically, indicating that smaller stingless bees have proportionally larger wings. All multispecies regression lines were plotted with PGLS.

were captured in Gamboa, Panamá, while *T. muzoensis*, and *P. frontalis* were collected on Barro Colorado Island. *Melipona triplaridis*, *S. panamensis*, and *L. danunica* were collected from the property of David Roubik in Curundu, Panamá, and *P. franki* and *M. panamica* were captured at the Santa Rita Arriba property of David Roubik. In each case, foragers were identified and captured as they returned to the nest from a single colony of each species. Another two species (13 in total), *Trigonisca atomaria* and *T. buoyssoni*, were collected while foraging at flowers using the canopy crane at Parque Natural Metropolitano, Panama City, Panamá, and at Santa Rita Arriba while foraging honey water. Individuals were placed in 50 mL tubes with sugar water on cotton for food if they could not be measured within 1 h of capture due to transportation time constraints. All bees were brought back to the Smithsonian Tropical Research Institute (STRI) lab in Gamboa, Panamá, for measurements. We verified the identities of all species using the STRI insect collection.

**Respirometry and wingbeat frequency analysis:** All bees were weighed on a Mettler-Toledo microbalance and placed in Fluon coated glass flight chambers for

flow-through respirometry. Ambient air was pushed through silica and soda lime scrubber columns by an aquarium pump, and flow rate through the respirometry chamber was adjusted using a Sable Systems Flow-Bar 8 mass-flow controller (resolution  $\pm 0.1$  mL min $^{-1}$  below 100 mL min $^{-1}$ ; resolution 1 mL min $^{-1}$  above 100 mL min $^{-1}$  flow rate). Excurrent CO<sub>2</sub> was measured using a LiCor 6252 plumbed in the differential mode (the reference cell measured the air flowing into the chamber and the sample cell measured air flowing out of the chamber; resolution was  $\sim 0.2$  ppm with hardware and software time-averaging of 1 s). The system was calibrated and spanned using a CO<sub>2</sub> tank containing 1221 ppm CO<sub>2</sub> (as measured by J. Shik with a LiCor 7000 calibrated against a certified span gas), with the zero-span reset each time the flow rate was changed and zeroed before and after each bee was measured. We used four different cylindrical glass flight chambers with volumes of 15, 70, 150, and 550 mL; chamber sizes were adjusted to the size of the bee. We chose the smallest chamber that a species would fly consistently in. Flow rates were adjusted to chamber size so that the 95% washout time for that chamber was  $\sim 1$  min or less; flow rates

ranged from 150 mL min<sup>-1</sup> for the smallest chambers to 1000 mL min<sup>-1</sup> for the largest chamber used. CO<sub>2</sub> levels during flight ranged from 6–175 ppm, with a minimal signal-to-noise ratio of 9.5. The analog outputs of the CO<sub>2</sub> analyzer and mass flow-controller were digitized and recorded with a Sable Systems (North Las Vegas, Nevada, USA) UI-2 and a computer using Sable Systems Expedata Pro 1.7.2 (digitization resolution was 0.5 ppm for the CO<sub>2</sub> analyzer, accounting for baseline noise, and 0.1 mL min<sup>-1</sup> for the mass flow-controller).

We used several methods to maintain good flight behavior, including agitation of the chamber and shining a bright light above the chamber while its surroundings were kept dark. We only accepted data from bees that exhibited at least 30 s of consistent flight behavior, which was accompanied by a relatively high and consistent CO<sub>2</sub> reading measured after the time required for washout of any atmospheric CO<sub>2</sub> that may have entered the chamber when the bee was placed inside (average flight duration measured was 43 s). After measuring CO<sub>2</sub> emission during flight, the air pump was turned off and we inserted a Sony ECM-PC60 mini electric condenser microphone to record wingbeat frequency for each bee. This was recorded and analyzed using Raven Lite 1.0 software. A subsample of 4–5 bees/species were then stimulated to fly in the same chambers and filmed with a Redlake (San Diego, CA, USA) MotionPro X high-speed video camera at 1000 fps to verify wingbeat frequency data acquired with the microphone. We used the average wingbeat frequency from three measures per individual for analysis. Air temperatures during the flight studies ranged from 23.5 to 25.5°C.

**Body temperature in flight:** After measurements of wing beat frequency, we removed bees from the chamber and placed them in a plastic gallon Ziploc bag; they continued flying within the bag until the measurement of body temperature was accomplished. We used a “grab-and-stab” measurement technique (Roberts and Harrison 1999) with a Physitemp (Clifton, New Jersey, USA) MT-29/1 hypodermic needle microprobe (29 ga, 0.025 s time constant) and a Physitemp BAT-10 thermocouple meter. To minimize thermal transfer from human to bee, we wore insulated gloves to hold the temperature microprobe, and restrained bees by pulling the plastic bag tight about them, on top of a Styrofoam board. We measured air, abdomen, and head temperatures in random order for every bee after first measuring thorax temperature; thorax temperatures were taken within 1 s of restraint and all temperatures were measured within an additional 2 s, which minimized any heat transfer from the process. To confirm that we were able to accurately measure body temperatures on the small species, we measured body segment temperatures of 10 recently killed bees of each

species that had been kept in an incubator at 25 or 30°C, using identical methods as for the live bees. The body temperatures of the dead bees that we measured were within 0.4°C of incubator temperatures, verifying that we did not warm the bees by handling or with the thermocouple, and that these bees did not cool too rapidly for accurate measurement.

We also flew 30 *S. luteipennis* (a medium sized species) individuals at temperatures between 25 and 40°C to establish a  $Q_{10}$  for flight metabolic rate, which was 0.96 on average. Each bee was placed in a Fluon-lined respirometry chamber (as outlined above) that was located inside the chamber with foam insulation and plastic sheeting in front to access the flight chamber. We used an ITC-306T Inkbird Temperature Controller (Inkbird, Shenzhen, China) probe, and connected the controller to a heater and fan that kept the temperature constant within the chamber ( $\pm 0.5^\circ\text{C}$ ) while the bee was flying. A micro thermocouple probe was also placed inside the respirometry chamber to record temperature during flight. We flew each bee at a single air temperature and made a thermal performance curve (Fig. 2C) with data from all bees and then calculated  $Q_{10}$ .

**Wing morphology and load carriage:** We removed the wings for 10 individuals/species by removing and flattening them onto white cardstock paper with transparent tape. A digital image of each wing was taken with a 1 mm grid for calibrating measurements. All measurements were performed in ImageJ. To determine load carriage (the maximum amount of liquid that could be carried), we starved 10 bees per species for 2 h, weighed them, then fed them 50% sucrose solution to satiation, weighed them, and encouraged them to fly as described above. If they would not fly, we continued coaxing them until they would and immediately reweighed at that time to reflect the most accurate load they could lift off and fly with.

**Phylogenetic and statistical Analysis:** All data for stingless bees are represented as species means  $\pm$  SE (standard error) of individual measurements. The effect of body mass was tested using least squares linear regression performed on log-transformed data to obtain the metabolic rate equation  $aM^b$ , where  $a$  =  $y$ -intercept,  $M$  = body mass, and  $b$  = allometric scaling coefficient (Darveau et al. 2005).

We converted metabolic rates (mL g<sup>-1</sup> h<sup>-1</sup>) to watts and applied corrections for various  $Q_{10}$  values [ $Q_{10} = 1$  as measured in *S. luteipennis* (Fig. 2C) and  $Q_{10} = 2$ , which is more typical of hymenopterans] to compare with flight metabolic rate data from the literature (Fig. 1D). We assumed RQ = 1 based on available data for hymenopterans (Suarez et al. 2005) and because bees were fed solely on a diet of sucrose water while in captivity. Further analyses of wingbeat frequency,

**Table 1** PGLS statistics for all physiological variables for 13 species of stingless bees.

Measurement	Slope	Intercept	t	P	Adj. $r^2$	$\lambda$	Conf. limits
Flight MR ( $\text{CO}_2\text{mLh}^{-1}$ )	<b>2.234</b>	2.843	14.466	<b>1.668e-08*</b>	0.946	0.000	0.274
Head temp ( $^{\circ}\text{C}$ )	0.225	0.804	1.828	0.095	0.163	0.490	0.219
Thorax temp ( $^{\circ}\text{C}$ )	<b>0.298</b>	1.043	2.466	<b>0.032*</b>	0.297	1.000	0.216
Abdomen temp ( $^{\circ}\text{C}$ )	0.146	0.578	1.322	0.213	0.059	0.570	0.198
Wing beatfreq (Hz)	0.015	2.323	0.430	0.675	-0.073	0.000	0.062
Load carriage (mg)	0.869	0.776	15.666	<b>7.693e-08*</b>	0.967	0.000	0.100
Forewing area ( $\text{mm}^2$ )	<b>0.499</b>	0.431	8.749	<b>2.762e-06*</b>	0.863	0.898	0.119
Total wing area ( $\text{mm}^2$ )	0.567	1.869	8.308	<b>4.55e-06*</b>	0.850	0.832	0.121
Hindwingarea ( $\text{mm}^2$ )	0.643	1.639	9.757	<b>9.449e-07*</b>	0.887	1.000	0.118
Forewing width (mm)	<b>0.269</b>	0.783	8.234	<b>4.963e-06*</b>	0.848	0.860	0.059
Forewing length (mm)	0.301	1.281	7.767	<b>8.646e-06*</b>	0.832	0.842	0.069
Hindwinglength (mm)	0.314	1.147	8.459	<b>3.826e-06*</b>	0.855	0.775	0.066
Hindwingwidth (mm)	0.315	0.585	8.110	<b>5.733e-06*</b>	0.844	0.904	0.069
Head mass (mg)	<b>0.860</b>	-0.921	9.839	<b>4.097e-06*</b>	0.906	0.000	0.155
Abdomen mass (mg)	1.109	-0.485	7.906	<b>2.431e-05*</b>	0.860	0.567	0.212
Thorax mass (mg)	1.046	-0.235	9.275	<b>6.668e-06*</b>	0.895	0.858	0.201

All scaling data were regressed using PGLS as part of the regression model, which integrates linear models to fit a line based on evolutionary relatedness through data. Phylogenetic signal ( $\lambda$ ) is on a 0–1 scale where 1 is the highest amount of signal possible. Coefficient t measures the distance of the line estimate (slope) from zero, with higher number demonstrating higher significance of the relationship between variables (body mass and the physiological variables shown). Slopes indicated in bold indicate nonisometric scaling. For flight MR and masses, the predicted isometric slope = 1; for temperatures and frequencies, the predicted isometric slope = 0; for widths and lengths, the predicted isometric slope = 0.33; and for areas, the predicted isometric slope = 0.67. Bolded P values indicate the slope is statistically different from zero. Confidence limits for the slopes are shown with 12 df (13 species included in analysis).

wing area, wing loading, and flight body temperature were performed using phylogenetic generalized least squares regressions (PGLS) in R on log-transformed data. A comprehensive maximum-likelihood tree based on [Rasmussen and Cameron \(2010\)](#) and [Ramirez et al. \(2010\)](#) was adapted for this study by pruning unnecessary species and adding species that did not appear on the published phylogenies. Branch lengths for all tip species were then set equal to 1 ([Rasmussen and Cameron 2007, 2010; Ramirez et al. 2010; Garamszegi 2014](#)). PGLS was performed for all analyses using all statistically possible tree topologies and results were obtained using the topology with the highest likelihood ([Garamszegi 2014](#)).

We compared the known metabolic rates of 117 flying insects by compiling literature values ([Supplementary Table S1](#)). Data points were eliminated from this dataset if they did not use modern methods (i.e., flow-through or stop flow respirometry) for determining flight metabolic rates or were measured in non-standard conditions (i.e., fluctuating temperatures or humidity, dietary manipulations, carried loads, etc.). We generated all possible models for flight metabolic rate scaling, including breakpoint models of log body mass vs. log metabolic, in R using the breakpoints and lm.br packages ([Priyadarshana and Sofronov 2016](#)). The model

was unconstrained to allow discontinuous slopes on either side of breakpoints and bootstrap restart sampling between 20 and 60 mg body mass. This generated multiple possible piece-wise regressions that differed in slope and breakpoint. We chose the regression with the lowest error represented as MSE. We compared this piece-wise regression to the standard models with a continuous slope across body size of 0.75 and 1.0 using Akaike's information criterion (AIC) comparisons from the breakpoints package in R.

## Results and discussion

Flight metabolic rates scaled hypermetically across stingless bee species, with a scaling exponent of 2.25 ([Fig. 2B](#),  $\text{Adj. } R^2 = 0.66$ ,  $P < 0.001$ ,  $\lambda = 0.00$ ,  $P_{(0)} = 0.0175$ ). This slope was not significantly affected by corrections using PGLS analysis ([Table 1](#)). The 95% confidence limits for this slope did not include isometry (slope = 1) or the hypometric exponents found for Euglossine bees or moths ([Bartholomew and Casey 1977, 1978; Dillon and Dudley 2004](#)). The different scaling patterns in Euglossines and stingless bees are not due to differences in absolute cost, since at body masses at which both taxa have been measured (circa 100 mg) flight metabolic rates are very similar ([Fig. 2B](#)).

Flight muscles of insects generate substantial heat, and most insects  $>50$  mg fly at thorax temperatures 5–20°C above air temperature, while insects with body masses  $<50$  mg have high cooling rates due to their higher surface-to-volume ratios, and usually have body temperatures close to air temperature (May 1981; Unwin and Corbet 1984; Heinrich 1993). Body temperatures of stingless bees demonstrated the size-related pattern expected from studies of other insects (Fig. 2C and D). Stingless bees heavier than 70 mg (*M. panamica* and *M. triplaridis*) had substantially elevated body temperatures, more than 10°C above air temperature, as previously shown (Roubik and Peralta 1983). In these two large species, thorax temperatures were the highest, as predicted by heat production in the flight muscles, and the abdomen was the coolest region (Fig. 2E). In contrast, in stingless bee species  $<20$  mg, head, thorax, and abdomen temperatures were mostly uniform and only about 1–3°C above air temperature (Fig. 2D).

Might the thermal differences between large and small bees drive the hypermetric scaling of flight metabolic rates in stingless bees, with the warmer temperatures of larger bees allowing higher metabolic rates? The metabolic rates of large flying insects can increase with thorax temperature (Heinrich 1971; Harrison et al. 2001), decrease with thorax temperature (Byrne et al. 1988; Harrison et al. 1996; Roberts and Harrison 1999), or be independent of thorax temperature (Heinrich and Casey 1973; Bartholomew and Casey 1977; Casey 1981, 1989; May 1995), depending on the species and range of thorax temperatures examined. We found a  $Q_{10}$  of 0.96 in one species of stingless bee (*S. luttipennis*) with no significant trend in flight metabolism over a 20°C range of thorax temperatures (Fig. 2D). If this low thermal sensitivity of flight applies to all species, then variation in body temperature will not explain variation in flight metabolism. However, for the small insects that have been measured, flight performance increases strongly over cool to moderate ranges of thoracic and air temperature, with  $Q_{10}$  values for wing beat frequency, flight speed, force production, power output, and metabolic rates of 1.2–2 (Yurkiewicz and Smyth 1966; Heinrich 1975; Lehmann 1999; Henry and Harrison 2014). To test the possibility that the lack of hypometric scaling of stingless bees was caused by thermal variation across species, we fit the thorax temperature data with a third-order polynomial (Fig. 2C), and then used these data to apply  $Q_{10}$  corrections to the flight metabolic data (Fig. 2B). Using a  $Q_{10}$  correction of 2, one of the highest  $Q_{10}$  values found for flying insects, the scaling slope was still significantly hypermetric with a slope of 2.11 (Fig. 2B, Table 1). Thus, the lack of hypometric scaling in flying stingless bees cannot be explained by thermal variation among these species.

The differential scaling of flight metabolic rates in stingless bees and Euglossine bees was associated with differential scaling of their wing morphology. Larger stingless bees had relatively smaller forewings, as the slope of total forewing area scaled with body mass with a scaling exponent of 0.50 (Fig. 2F, Table 1), significantly less than the isometric prediction of 0.67. Hind-wing area and total wing area scaled isometrically. In contrast, in Euglossine bees, larger bees have relatively larger wings than predicted by isometry (Casey et al. 1985). The relatively smaller forewing area in larger stingless bees arose mostly from these wings being relatively narrower (Fig. 3, Table 1), as wing lengths scaled isometrically (Fig. 3). One possibility is that the relatively larger forewings in smaller bees could create more lift per stroke, potentially reducing energetic cost and contributing to the lower flight cost per gram observed in smaller bees.

In contrast to the scaling of wing area, the masses of body segments scaled similarly to other insects. Stingless bee thorax mass scaled about isometrically (slope = 1.05 Adj.  $R^2 = 0.895$ ,  $\lambda = 0.858$  [Table 1]), consistent with orchid bees (probably the most studied group of for flight physiology) and other bees and insects measured (Dillon and Dudley 2004; Darveau et al. 2005). Abdomen mass also scaled isometrically (slope = 1.11 Adj.  $R^2 = 0.86$ ,  $\lambda = 0.567$  [Table 1]) and head mass scaled hypometrically (slope = 0.86, Adj.  $R^2 = 0.906$ ,  $\lambda = 0.00$  [Table 1]) as found for other insects and vertebrates (Darveau et al. 2005; Eberhard and Wcislo 2011; Grula et al. 2021).

The differential scaling of flight costs in stingless and Euglossine bees was also supported by differential scaling of wing beat frequencies in these groups. In a strikingly different pattern from that observed for fliers with larger masses, wing beat frequency was independent of mass (Figs. 2F and 3C). Most studies of insects have found that wing beat frequencies decrease with increasing body mass. For example, in Euglossines, the scaling exponent for wing beat frequency was  $-0.31$  (Roberts et al. 1998). However, our results for a differential scaling of wing beat frequencies in smaller insects are supported by Byrne (1988), who demonstrated that aphids and white flies  $<30$  mg do not demonstrate reduced wingbeat frequencies in the larger species.

As for most other fliers studied (Marden 1994; Lehmann 1999, 2009), bees lifted similar fractions of their body mass during voluntary load-lifting of nectar, despite their varied thorax temperatures and hypermetric scaling of costs of flight when not loaded. Similarly, using a progressive load-lifting method, Dillon and Dudley found that vertical force production scaled either isometrically (using log-transformed data) or hy-

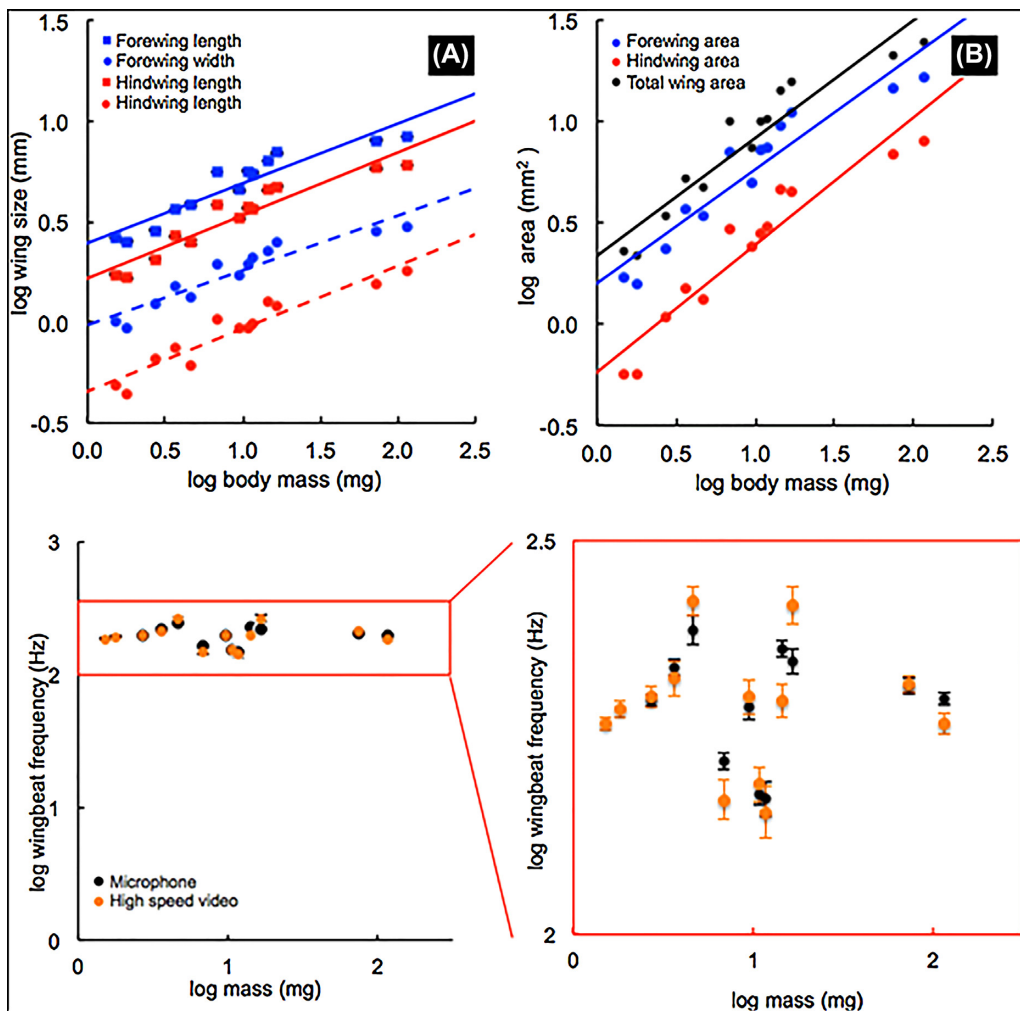


**Fig. 3** (A) Scaling relationships of forewing (blue) and hindwing (red) length (squares), and widths (circles). All scaled isometrically with body mass (Table 1). (B) Scaling of total wing area (black), forewing area (blue), and hindwing area (red) with body mass. Forewings are proportionally larger in smaller bees than hindwings. All scaling parameters are listed in Table 1. (C) Comparison of microphone and high-speed video methods of wing beat frequency measurement. There was no significant relationship between mass and wing beat frequency among all species (slope = 0.02, Adj.  $R^2$  = 0.066,  $P$  = 0.524). Average wing beat frequency across species =  $204.6 \pm 8.3$  SE beats  $s^{-1}$ . Each point represents the average wing beat frequency within a species  $\pm$  SE.

pometrically (using raw data) across Euglossine bees (Dillon and Dudley 2004). Thus, smaller stingless bees can carry similar loads (mass-specifically) at reduced cost relative to larger stingless bees. This pattern is may be partially due to the fact that smaller bees had relatively larger forewings (Fig. 3B).

Finally, we combined our data with all currently published data on flight metabolic rates of hovering insects to synthesize the scaling of flight costs across this clade (Supplementary Table S1). The flight metabolic rates of stingless bees closely approximated costs of other similarly sized insects (Fig. 4). Inspection of all insect flight metabolic rates indicated that there was a breakpoint in the scaling of metabolic rates with size; a breakpoint analysis indicated that the breakpoint occurred at 58 mg (Fig. 4). A biphasic model using two

size classes ( $>58$  mg and  $<58$  mg) better explained the scaling of metabolic rates than a simple continuous log-log model, based on the residual MSE of the generated breakpoint models compared to the standard model (Table 2). We next fit linear models to log-log plots of metabolic rates vs. mass  $>58$  mg and  $<58$  mg; these had high  $r^2$  values, particularly in the low range, (Table 2). The scaling slope of flight metabolic rate below 58 mg was 1.199, and 0.675 above 58 mg (Fig. 4). We conclude that scaling of insect flight metabolic rates is biphasic, with hypermetric scaling in the low size range and hypometric scaling in the high size range.

The mechanisms responsible for the biphasic scaling of flight costs remain unclear, but likely include both aerodynamic and evolutionary mechanisms, probably

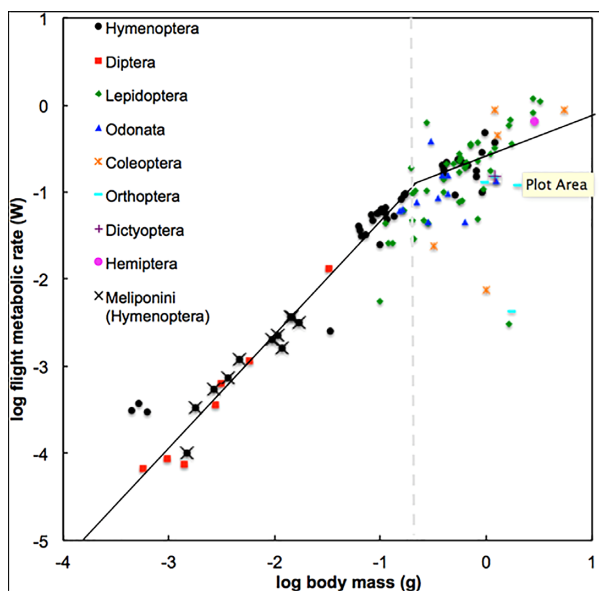


**Fig. 4** The effect of size on the scaling of flight metabolic rate depends on the body size range examined (Table 2). Flight metabolic rate in insects  $<58$  mg in body mass scales hypermetically (slope = 1.19), indicating that mass-specific costs are less for smaller insects in this size range. In contrast, for insects  $>58$  mg in body mass, flight metabolic rate scales hypometrically (slope = 0.67), with higher mass-specific costs for smaller animals, as has been observed among flying vertebrates.

working together. Aerodynamic costs of flight may be reduced among smaller insects, due partly to performance at low Reynolds numbers. At lower Reynolds numbers, less energy may be required for flight because the relatively increased air viscosity experienced by smaller flyers reduces lift requirements (effectively increasing “buoyancy” of smaller animals). This increased buoyancy is illustrated by the fact that insects further order of magnitude smaller than these stingless bees have evolved decreased wing veination or “feather” wings that allow them to float through air rather than actively flying (Farisenkov 2020). In the large size range of insects  $>58$  mg, and all vertebrate fliers, smaller species must use higher wing-beat frequencies than larger species to generate sufficient mechanical power to hover, and these higher frequencies

lead to higher mass-specific costs due to higher ATP use by the myosin and  $\text{Ca}^{++}$  ATPases (Biewener and Patek 2018). In contrast, in the size range  $<58$  mg, higher relative buoyancy may allow smaller insects to conserve energy because they do not need to increase wing beat frequencies to generate sufficient lift. Additionally, evolutionary changes in morphology may reduce the mass-specific cost of flight in smaller stingless bees. Smaller stingless bees have relatively larger wings (Fig. 3), as well as decreased veination on the laminar surface of the forewing, a relatively larger stigma, and a heavier forewing leading edge (Danforth 1989; Combes and Daniel 2003; Nel et al. 2012). These characteristics may provide greater lift generation, further enabling smaller species to fly without requiring energetically expensive increases in wing beat frequency. Smaller stingless bees also have proportionally larger heads; this contributes to a shift in the center of mass to a more forward position (Ellington 1984; Liu 2009). Such morphological changes may contribute to using different aerodynamic mechanisms, such as “clap and fling” found in some tiny species (Miller and Peskin 2009; Farisenkov et al. 2020). Regardless of the mechanism, the reduced cost of flight at sizes  $<58$  mg will likely reduce costs of flight for foraging, defense, and migration, providing a significant selective advantage for the evolution of small body size among insects. However, it should be noted that these reduced costs for small insect fliers applies to hovering flight as studied here, when costs of generating lift predominate. During forward flight, drag forces on the body become important, and the low Reynold’s number and high surface-to-volume ratios of smaller insects may cause an increase in flight costs (Ellington 1985, 1999; Fry et al. 2005).

The biphasic scaling of flight metabolic rates in insects seems to contradict predictions of hypotheses for metabolic scaling that depend on supply constraints in larger animals. Also, this biphasic pattern further reinforces the growing consensus that scaling patterns are variable with clade and type of activity. At least for insect hovering flight at body masses from 1 to 1000 mg, our data support the hypothesis that patterns of metabolic scaling are determined by changes in the aerodynamic

**Table 2** Comparison of most likely linear and breakpoint models for flight metabolic rate scaling across flying insects.

Model	Slope	St. Err.	P (slope = 0)	P (slope = 0.67)	P (slope = 1)	Intercept	$\Theta$	AIC	Akaike weight
Linear	0.98	0.04	<0.001*	<0.001*	0.562	-0.62	NA	139.03	0.003
Break-point	Left: 1.19	0.07	<0.001*	<0.001*	<b>0.027*</b>	-1.03	-0.63	127.34	0.997
	Right: 0.67	0.17	<b>0.004*</b>	0.305	<b>0.004*</b>				

The breakpoint model has much higher support using AIC than the standard linear model.

cost of locomotion, and changes in skeletal muscle cycle frequency.

## Acknowledgments

We acknowledge Panama's Ministerio de Ambiente and the Smithsonian Tropical Research Institute (STRI) for permitting and aiding in this research. We are especially grateful to the following individuals at STRI for logistical and technical support: Bill Wcislo, Jon Shik, Lil Camacho, Raineldo Urriola, Paola Galgani, Vilma Fernandez, and Oris Acevedo. We are also grateful to Josh Borup, who contributed to wing morphology data collection.

## Funding

This work was supported by the Society of Integrative and Comparative Biology (SICB), the National Science Foundation (grant number IOS 1122157 to J.F.H.), and the Smithsonian Tropical Research Institute.

## Supplementary data

Supplementary Data available at [ICB](#) online.

## Conflict of Interest

The authors state that they have no conflicts of interest related to this paper.

## Data availability

All data used in this publication are available at <https://doi.org/10.5061/dryad.g1jwstqtf>.

## References

Bartholomew GA, Casey TM. 1978. Oxygen consumption of moths during rest, pre-flight warm-up, and flight in relation to body size and wing morphology. *J Exp Biol* 76:11–25.

Bartholomew GA, Casey TM. 1977. Body temperature and oxygen consumption during rest and activity in relation to body size in some tropical beetles. *J Therm Biol* 2:173–6.

Biewener A, Patek S. 2018. Animal locomotion. Oxford, U.K.: Oxford University Press.

Byrne DN, Buchman SL, Spangler HG. 1988. Relationship between wing Loading, wingbeat frequency and body mass in Homopterous insects. *J Exp Biol* 135:9–23.

Cardoso JFMF, van der Veer HW, Kooijman SALM. 2006. Body-size scaling relationships in bivalve species: a comparison of field data with predictions by the Dynamic Energy Budget (DEB) theory. *J Sea Res* 56:125–39.

Casey TM. 1981. Energetics and thermoregulation of *Malacosoma americanum* (Lepidoptera: Lasiocampidae) during hovering flight. *Physiol Zool* 54:362–71.

Casey TM. 1989. Oxygen consumption during flight. In: Goldsworthy GJ, Wheeler CH, editors. *Insect flight*. Boca Raton: CRC Press. p. 257–72.

Casey TM, May ML, Morgan KR. 1985. Flight energetics of Euglossine bees in relation to morphology and wing stroke frequency. *J Exp Biol* 116:271–89.

Combes SA, Daniel TL. 2003. Flexural stiffness in insect wings I. Scaling and the influence of wing venation. *J Exp Biol* 206:2979–87.

Danforth BN. 1989. The evolution of hymenopteran wings: the importance of size. *J Zool* 218:247–76.

Darveau CA, Hochachka PW, Welch KC, Roubik DW, Suarez RK. 2005. Allometric scaling of flight energetics in Panamanian orchid bees: a comparative phylogenetic approach. *J Exp Biol* 208:3581–91.

de Camargo JMF. 2013. Historical biogeography of the Meliponini (Hymenoptera, Apidae, Apinae) of the neotropical region. In: Vit P, Pedro SRM, Roubik DW, editors. *Pot honey: a legacy of stingless bees*. Berlin, Germany: Springer Nature. p. 19–34.

de Camargo JMF, Pedro SRM. 2013. Meliponini, Lepeletier 1836. In: Moure JS, Urban D, Melo GAR, editors. *Catalogue of Bees (Hymenoptera, Apoidea) in the neotropical region*. Sociedade Brasileira de Entomologia, Curitiba, PR, Brasil.

Dillon ME, Dudley R. 2004. Allometry of maximum vertical force production during hovering flight of neotropical orchid bees (Apidae: Euglossini). *J Exp Biol* 207:417–25.

Eberhard WG, Wcislo WT. 2011. Grade changes in brain-body allometry: morphological and behavioural correlates of brain size and miniature spiders, insects and other invertebrates. *Adv Insect Physiol* 40:155–214.

Ellington CP. 1984. The aerodynamics of hovering insect flight. III. Kinematics. *Philos Trans R Soc Lond* 305:41–78.

Ellington CP. 1985. Power and efficiency of insect flight muscle. *J Exp Biol* 115:293–304.

Ellington CP. 1999. The novel aerodynamics of insect flight: applications to micro-air vehicles. *J Exp Biol* 202: 3439–48.

Farisenkov SE, Lapina NA, Petrov PN, Polilov AA. 2020. Extraordinary flight performance of the smallest beetles. *Proc Natl Acad Sci* 117:24643–5.

Felsenstein J. 1985. Phylogenies and the comparative method. *Am Nat* 125:1–15.

Fry SN, Sayaman R, Dickinson MH. 2005. The aerodynamics of hovering flight in *Drosophila*. *J Exp Biol* 208:2303–18.

Garamszegi LZ. 2014. Modern phylogenetic comparative methods and their application in evolutionary biology: concepts and practice. Berlin: Springer-Verlag.

Grula CC, Rinehart JP, Greenlee KJ, Bowsher JH. 2021. Body size allometry impacts flight-related morphology and metabolic rates in the solitary bee *Megachile rotundata*. *J Insect Physiol* 133:104275.

Harrison JF, Camazine S, Marden JH, Kirkton SD, Rozo A, Yang X. 2001. Mite not make it home: tracheal mites reduce the safety margin for oxygen delivery of flying honeybees. *J Exp Biol* 204:805–14.

Harrison JF, Fewell JH, Roberts SP, Hall HG. 1996. Achievement of thermal stability by varying metabolic heat production in flying honeybees. *Science* 274:88–90.

Harrison JF, Roberts SP. 1998. Mechanisms of thermoregulation in flying bees. *Am Zool* 38:492–502.

Harvey PH, Pagel MD. 1991. The comparative method in evolutionary biology. New York (NY): Oxford University Press.

Heinrich B. 1971. Temperature regulation of sphinx moth, *Man-  
duca sexta* 1. Flight energetics and body temperature during  
free and tethered flight. *J Exp Biol* 54:141–52.

Heinrich B. 1975. Thermoregulation in bumblebees II. Ener-  
getics of warm-up and free flightH. *J Comp Physiol B* 96:  
155–66.

Heinrich B. 1993. The hot-blooded insects. Cambridge (MA):  
Harvard University Press.

Heinrich B, Casey TM. 1973. Metabolic rate and endothermy in  
sphinx moths. *J Comp Physiol* 82:195–206.

Henry JR, Harrison JF. 2014. Effects of body size on the oxygen  
sensitivity of dragonfly flight. *J Exp Biol* 217:3447–56.

Lehmann F-O. 1999. Ambient temperature affects free-flight per-  
formance in the fruit fly *Drosophila melanogaster*. *J Comp  
Physiol B Biochem Syst Environ Physiol* 169:165–71.

Lehmann F-O. 2009. Wing-wake interaction reduces power  
consumption in insect tandem wings. *Exp Fluids* 46:  
765–75.

Liu H. 2009. Integrated modeling of insect flight: from mor-  
phology, kinematics to aerodynamics. *J Comput Phys* 228:  
439–59.

Marden JH. 1994. From damselflies to pterosaurs: how burst and  
sustainable flight performance scale with size. *Am J Physiol  
Regul Integr Comp Physiol* 266:R1077–84.

May ML. 1981. Wingstroke frequency of dragonflies (Odonata:  
Anisoptera) in relation of temperature and body size. *J Comp  
Physiol B* 144:229–40.

May ML. 1995. Dependence of flight behavior and heat produc-  
tion on air temperature in the green garner dragonfly *Anax  
junius* (Odonata: Aeshnidae). *J Exp Biol* 198:2385–92.

Michener CD. 2001. Comments on minute Meliponini and the  
male of the genus *Pariotrigona* (Hymenoptera: Apidae). *J Kans  
Entomol Soc* 74:231–6.

Miller LA, Peskin CS. 2009. Flexible clap and fling in tiny insect  
flight. *J Exp Biol* 212:3076–90.

Nel A, Prokop J, Nel P, Grandcolas P, Huang D-Y, Roques P,  
Guilbert E, Dostál O, Szwedo J. 2012. Traits and evolution  
of wing venation pattern in paraneopteran insects. *J Morphol*  
273:480–506.

Nisbet RM, Muller E, Lika S, Koojiman SALM. 2000. From  
molecules to ecosystems through dynamic energy budget  
models. *J Anim Ecol* 69:913–26.

Niven JE, Scharlemann JPW. 2005. Do insect metabolic rates at  
rest and during flight scale with body mass? *Biol Lett* 1:346–9.

Priyadarshana W, Sofronov G. 2016. breakpoint: an R pack-  
age for multiple break-point detection via the cross-entropy  
method. <https://rdrr.io/cran/breakpoint/man/breakpoint-package.html>. 1-2016

Ramírez SR, Nieh JC, Quental TB, Roubik DW, Imperatriz-  
Fonseca VL, Pierce NE. 2010. A molecular phylogeny of the  
stingless bee genus *Melipona* (Hymenoptera: Apidae). *Mol  
Phylogen Evol* 56:519–25.

Rasmussen C, Cameron SA. 2007. A molecular phylogeny  
of the Old World stingless bees (Hymenoptera: Apidae:  
Meliponini) and the non-monophyly of the large genus *Trig-  
ona*. *Syst Entomol* 32:26–39. <https://doi.org/10.1111/j.1365-3113.2006.00362.x>

Rasmussen C, Cameron SA. 2010. Global stingless bee phylogeny  
supports ancient divergence, vicariance, and long distance dis-  
persal. *Biol J Linn Soc* 99:206–32.

Roberts SP, Harrison JF. 1999. Mechanisms of thermal stabil-  
ity during flight in the honeybee *Apis mellifera*. *J Exp Biol*  
202:1523–33.

Roberts SP, Harrison JF, Hadley NF. 1998. Mechanisms of  
thermal balance in flying *Centris pallida* (Hymenoptera: Anthophoridae). *J Exp Biol* 201:2321–31.

Roubik DW, Peralta FJA. 1983. Thermodynamics in nests of two  
*Melipona* species in Brasil. *Acta Amaz* 13:453–66.

Sibley RM, Brown JH, Kodric-Brown A. 2012. Metabolic ecology:  
a scaling approach. Wiley-Blackwell: New York, N.Y., USA.

Suarez RK. 2000. Energy metabolism during insect flight:  
biochemical design and physiological performance. *Physiol  
Biochem Zool* 73:765–71.

Suarez RK, Darveau CA, Hochachka PW. 2005. Roles of hier-  
archical and metabolic regulation in the allometric scaling of  
metabolism in Panamanian orchid bees. *J Exp Biol* 208:3603–  
7.

Unwin DM, Corbet SA. 1984. Wingbeat frequency, temperature  
and body size in bees and flies. *Physiol Entomol* 9:115–21.

West GB, Brown JH, Enquist BJ. 1997. A general model for the  
origin of allometric scaling laws in biology. *Science* 276:122–  
6.

Yurkiewicz WJ, Smyth T. 1966. Effect of temperature on flight  
speed of the sheep blowfly. *J Insect Physiol* 12:189–94.